Thin films of cross-linked polylactic acid as tailored platforms for controlled drug release

Zdeněk Krtouš, Jaroslav Kousal, Jana Sedlaříková, Zuzana Kolářová Rašková, Liliana Kučerová, Ivan Krakovský, Jaromír Kučera, Suren Ali-Ogly, Pavel Pleskunov, Andrei Choukourov

PII: S0257-8972(21)00576-4

DOI: https://doi.org/10.1016/j.surfcoat.2021.127402

Reference: SCT 127402

To appear in: *Surface & Coatings Technology*

Received date: 12 January 2021

Revised date: 11 May 2021

Accepted date: 3 June 2021

Please cite this article as: Z. Krtouš, J. Kousal, J. Sedlaříková, et al., Thin films of cross-linked polylactic acid as tailored platforms for controlled drug release, *Surface & Coatings Technology* (2021), https://doi.org/10.1016/j.surfcoat.2021.127402

Thin films of cross-linked polylactic acid as tailored platforms for controlled drug release

Zdeněk Krtouš[1], Jaroslav Kousal[1,2] *, Jana Sedlaříková[3,4], Zuzana Kolářová Rašková[4], Liliana Kučerová[3,4], Ivan Krakovský[1], Jaromír Kučera[2], Suren Ali-Ogly[1], Pavel Pleskunov[1] and Andrei Choukourov[1]

[1] Faculty of Mathematics and Physics, Charles University, V Holešovickách 2, 180 00 Prague, Czech Republic

[2] Faculty of Mechanical Engineering, Czech Technical University in Prague, Karlovo náměstí 13, 121 35 Prague, Czech Republic

[3] Faculty of Technology, Tomas Bata University in Zlín, Vavrečkova 275, 76001 Zlín, Czech Republic

[4] Centre of Polymer Systems, Tomas Bata University in Zlín, Třída Tomáše Bati 5678, 76001 Zlín, Czech Republic

* Correspondence: jaroslav.kousal@mff.cuni.cz

Abstract

Drug-loaded polymers are desirable for the controlled administration of bioactive molecules to biological media because polymer viscoelasticity can be translated into benefits of tissue-contacting materials. Here, we report on plasma-assisted deposition of polyester thin films performed via thermal evaporation of polylactic acid (PLA). The films can be produced with the chemical composition and polymer topology precisely tuned by the discharge power. At low power, weakly cross-linked films are produced with the chemical motif resembling that of PLA, the molar mass distribution peaking at ~350 g mol^{-1} and skewing to larger species. At high power, highly cross-linked films are produced with a worse resemblance to PLA. The films swell and dissolve in water, releasing oligomers with the dissolution kinetics spanning over a broad time scale of 10^{-1} – 10^{4} seconds. The released oligomers undergo hydrolysis at the time scale of days and with the final product of lactic acid, meeting the biocompatibility demands. When dissolving, the films expose micrometre-sized pores or buckling instabilities, depending on the discharge power. The phenomenon can be used for controlled release of nisin, an antibacterial peptide so that an hour-delayed release is achieved via the pore-mediated diffusion, whereas a minute-delayed release is achieved through the buckling. Nisin-loaded polyester plasma polymer films are effective against *Micrococcus luteus*, the bactericidal activity correlating with the drug release kinetics. Hence, the film design holds promise for developing advanced wound dressing materials and other tissue-contacting devices with tunable therapeutic effect.

Keywords

plasma polymerization, plasma-assisted vapour thermal deposition, polylactic acid, biodegradability, controlled drug release

ToC / Highlights

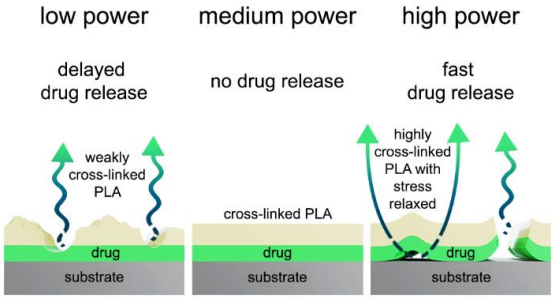

- Thin films of plasma polymers resembling classical polylactic acid were prepared.
- The timescale of dissolution can be tuned within several orders of magnitude.
- Two different mechanisms of degradation were observed.
- Control of kinetics of release of nisin from minutes to days was demonstrated.

1. Introduction

The development of efficient polymer-based drug delivery systems with controllable release kinetics has been intensively studied in recent years [1–5]. Several factors affecting the drug release have to be considered, such as polymer carrier character, polymer degradation rate, diffusion coefficient, or molecular weight of the incorporated drug [3]. Regarding suitable polymer matrix, biodegradable polyester-based materials, such as polylactic acid or poly(lactic-co-glycolic acid), have attracted many researchers [6–11]. Polylactic acid (PLA), belonging among the most extensively investigated renewable materials, can be applied in the biomedical field due to high biocompatibility, low level of toxicity, and suitable processing properties; for example, for the fabrication of absorbable sutures, medical implants, scaffolds, or drug delivery systems [12–16]. Understanding the mechanism of degradation is crucial to obtain an efficient platform for active molecules that should be released into a specific medium under given conditions [17].

The degradability of PLA is strongly affected by factors such as crystallinity, molecular weight, surface properties (wettability), temperature, pH, enzymatic activity, and the environment [18–20]. Different poly(L-lactide) degradation profiles were revealed in buffer solution versus 100 % relative humidity environment [17]. Belonging to polyesters, PLA exhibits poor hydrophilicity and low functionalization capability, which limits the practical applications. Various physical or chemical modifications have been studied to overcome some of these limitations and increase the hydrophilicity, adhesion and degradation profile [21]. Plasma treatment can ensure functionalization, leading to the change in surface roughness and morphological properties so that wettability and hydrophilicity are enhanced. Moreover, functional groups may serve as anchors for specific binding of the bioactive molecules with their subsequent release in a controllable manner [1,2,22–26].

Since standard chemical vapour deposition methods proceed at high temperatures, they are not suitable for thin films applied in biomedicine. On the other hand, plasma-enhanced chemical vapour deposition (PECVD) can be utilized to manufacture thin films and nanoparticles at lower temperatures [3,27–34]. However, this technique suffers from the fact that only low molecular weight substances can be used, restricting the potential scale of resultant plasma polymers though the retention of the monomer properties can be increased e.g. using pulsed plasma [35–38]. Plasma-assisted vapour (vacuum) thermal deposition (decomposition/degradation) (PAVTD) overcomes this limitation using polymer heating at reduced pressure and under an inert atmosphere. Compared to the PECVD technique, the PAVTD offers an attractive way to supply both low- and high-molecular-weight species to the gas phase. Such polydisperse species are then plasma-activated with the bond cleavage and radical formation, and undergo re-polymerization processes when deposited onto substrates [39–48]. An advantage of this method is that the structural properties can be easily controlled via the applied discharge power. As was shown for poly(ethylene oxide)-like PAVTD films, the release kinetics of bioactive nisin molecule was slowed down at higher plasma power, and undesirable burst effect was avoided [47]. Structurally, these films have been shown to cover the typical gap between classical and plasma polymers [48]. This paper aims to prepare PLA-based plasma polymer thin films with controllable hydrolysis, permeation, and adhesion, serving as platforms for the tunable release of bioactive molecules.

2. Materials and methods

Polylactic acid (PLA) of M_w = 10000–20000 g×mol^{-1} prepared by the procedure described in [17] was used as a source polymer for the PAVTD. Nisin standard from *Lactococcus lactis* was supplied by Sigma-Aldrich, USA. The substrates for the films were one side polished Si wafers, glass slides and wafers pre-coated with a gold layer.

2.1 PAVTD deposition

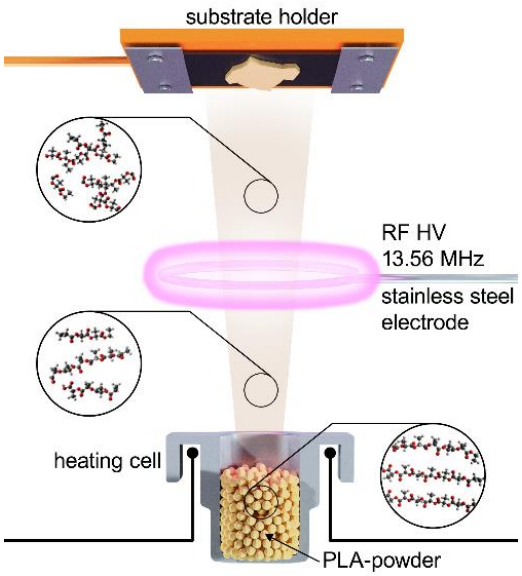

Figure 1 Scheme of the experimental PAVTD setup used to prepare plasma polymerized PLA thin films.

The setup for PAVTD [48] is schematically shown in Figure 1. The deposition system consisted of a stainless-steel vacuum chamber pumped down to base pressure 10^{-3} Pa by diffusion and rotary pumps. A tank with Ar was connected to the chamber (30 l volume, 300 mm diameter) via an automatic flow controller (MK1, MKS Instruments) to maintain a constant flow rate of 7 cm^3_{STP}/min and pressure of 5 Pa (measured by Type 626 Baratron, 266 Pa range, MKS). The chamber was rigged with a stainless-steel ring-shaped electrode 70 mm in diameter powered by a radio frequency (RF) power supply (Dressler Caesar, 13.56 MHz, Advanced Energy) via a matching unit. The power supply was operated in a continuous wave mode. An electrically heated (via molybdenum strips) copper crucible (height 33 mm, inner diameter 22 mm, outer diameter 28 mm) bearing PLA granules (2 grams per batch) was placed at a distance of 40 mm below the electrode. Quartz crystal microbalance sensor (QCM) monitored the deposition rate 100 mm above the electrode. The load-lock system was mounted to the chamber port transversally to maintain a 150 mm interspace gap between the sample holder and the crucible apex. The discharge was ignited, and the crucible with PLA load was heated up to the working temperature (~ 220°C) to produce the flux of PLA oligomers. Once the deposition rate was adjusted to the value of 5 nm/min, the substrates residing in the load-lock were introduced into the deposition chamber for 20 min. Finally, the substrates were retracted from the deposition chamber to the load-lock after the PLA thin films were deposited.

2.2 SEM

A Jeol JSM-7200F Scanning Electron microscope with a secondary electron detector was used with the acceleration voltage set at 2 KeV. No additional metallization was applied to the samples.

2.3 In-situ and ex-situ ellipsometry

The measurements were undertaken using a Woollam M-2000DI spectroscopic ellipsometer to obtain the thickness of the PLA plasma polymers. The measurements were performed on films deposited on polished silicon substrates. The *ex-situ* measurements were done at three angles ranging from 50° to 70° and in the wavelength range of 192 nm–1690 nm. The ellipsometry data were fitted using CompleteEASE software (J.A. Woollam) according to a Cauchy model for silicon substrate with 1.5 nm of native oxide.

The *in-situ* measurements were done in water using a liquid cell. The angle of measurements was fixed at 70°. The data were fitted by a Bruggeman effective medium approximation model, where the medium was water, and the polymer fraction was the layer described by the Cauchy model.

2.4 Infrared spectra (FTIR)

The FTIR measurements were performed in the reflection absorption configuration using a Bruker Equinox 55 spectrometer. The samples were deposited onto silicon substrates pre-coated by a gold-mirror film. The resolution was set at 4 cm^{-1}.

2.5 Thermal stability of the films

Thermal stability of the films was assessed by establishing the thickness ratio (measured by ellipsometry) before and after heating the samples under vacuum. The batch of samples was fixed on a heater plate and placed into a vacuum chamber with pressure below 2×10^{-3} Pa. The films were heated at a steady rate of 3.75 °C/min to the target temperature of 60 °C, 80 °C, 120 °C, 160 °C, 200 °C, and 230 °C, the latter corresponding to the PLA evaporation temperature. After reaching the target temperature, the samples were let cool down to 50 °C before venting the chamber. As a reference, the samples were heated to 30 °C and kept at this temperature under vacuum for 1 hour.

2.6 PLA hydrolysis

A hydrolysis test was carried out in demi water (enriched with 0.2 %wt. sodium azide) on the square-shaped glass samples (2.5x2.5 cm) that were previously subject to the PAVTD. The specimens were immersed into hydrolysis medium (at the temperature of 37 °C), placed into 20 ml weighing bottles, and agitated. At defined time intervals, an aliquot of 1 ml was withdrawn for LC-MS analysis performed on an Infinity LC System (Agilent Technologies, USA). Chromatographic separation was performed on an Extend column C18 (2.1x50 mm, 1 μm) at the flow rate of 0.5 $ml\times min^{-1}$. The mobile phase consisted of 0.1 % formic acid (A) and acetonitrile (B); the sample injection volume equalled to 1 μl. Standard of lactic acid (LA) was measured as a [M-H]- molecule ion, fragmentation of the precursor ion was carried out at 20 V.

2.7 Gel Permeation Chromatography

The distribution of the molar masses of the soluble fraction of the films was studied by the gel permeation chromatography (GPC) using an Agilent 1260 Infinity GPC/SEC system equipped with a differential refractometric detector. The samples were diluted as ca 3 % (w/v) solutions in tetrahydrofuran with a flow rate of 0.8 ml×min^{-1} at temperature 30 °C. The separation system with 0.2 μm Teflon membrane filter used a 7.5 x 600 mm Polymer Laboratories gel column of porosity 1000 Å calibrated with polystyrene standards.

2.8 Release of active molecules

Release experiment was carried out with nisin Mw ~3354 g×mol^{-1}. Active molecule-containing layers were prepared via spin-coating (3000 rpm) of the 450 ml total volume of polyvinyl alcohol (2 %wt.) solution with nisin (1 %wt.) on silicon wafers (2.5x2.5 cm). Subsequently, a PLA plasma polymer layer (thickness ~70 nm) was deposited over the active drug layer.

The samples containing nisin and PLA plasma polymers were immersed into demi water (at the temperature of 37 °C) in 20 ml weighing bottles and agitated. At defined time intervals, an aliquot of 1 ml was withdrawn for further analyses.

Detection of nisin was performed on an HPLC Shimadzu Prominence LC20A Series equipped with a thermostatted column compartment and a dual-wavelength UV-VIS detector (Shimadzu, Japan). The measurement was performed on an Aeris Widepore column XB-C8 (4.6x150 mm; 3.6 μm; Phenomenex, USA) at 40 °C. The mobile phase constituted a gradient composed of 0.1 % (v/v) HCOOH in HPLC grade water (solvent A) and HPLC grade acetonitrile (solvent B). Gradient elution was as follows: 0–13.5 min from 5.0 % eluent B to 40.0 % eluent B; 13.5–14.0 min from 40.0 % eluent B to 95.0 % eluent B; 14.0–18.5 min 95.0 % eluent B; 18.5–19.0 min from 95.0 % eluent B to 5 % eluent B; total run 25 min. Injection volume equalled to 40 μL, and the flow rate was set to 1.0 ml/min. Measurement was performed at the wavelengths of 200 and 220 nm; the nisin concentration was calculated from the 200 nm test results. Quantification of nisin was performed by an external calibration method, and the equation of the calibration curve was the following: y = 137970c + 159.26 (R^2 = 0.9992), where y represents the peak area and c is the concentration of nisin. All the experiments were carried out at room temperature.

2.9 Antibacterial tests

The samples were immersed in 15 ml of demineralized water at laboratory temperature. At defined time intervals, the aliquots of 1 ml were withdrawn and analyzed by an agar diffusion method using the bacterial suspension of *Micrococcus luteus*, CCM 732. One millilitre of bacterial suspension (the concentration from10^6 to 10^7 CFU×ml^{-1}) was transferred onto sterile Petri dishes with a Mueller Hinton agar. An eluate (100 μL) was placed into the bored wells of 8 mm in diameter and incubated at 30 °C. After the incubation period, the diameters of inhibition zones around the samples were recorded.

3. Results and discussion

3.1 Chemical composition and structure of the films

The PLA plasma polymers were deposited with different discharge powers, and their chemical composition was analyzed by FTIR (Figure 2). The spectra bear the characteristic features of PLA, including stretching vibrations of hydrocarbons at 2800–3000 cm^{-1}, carbonyls at 1730–1765 cm^{-1}, and other species at lower wavelengths [49,50]. If the spectra are normalized to carbonyl's absorbance, it becomes evident that the intensity of the hydrocarbon moieties increases with the plasma power, whereas the oxygen-bearing species subside. The phenomenon is further accompanied by a shift of the C=O peak from 1765 cm^{-1} to 1730 cm^{-1}, which is caused by changes in the local surroundings of the carbonyl groups. The shift to the lower wavenumber points to deoxidation of the local carbonyl environment with the replacement of oxygen atoms by carbonaceous species. The evolvement of a broad shoulder at 1650 cm^{-1} indicates that the C=C bonds may belong to these species, appearing as a result of the plasma-enhanced molecular fragmentation. These results are consistent with the earlier reports on the plasma-assisted deposition of poly(ethylene oxide)-like plasma polymers [40–42,47,48]. They also provide further evidence to a common idea of the enhancement of disorder in plasma polymers and overall loss of the original polymer's motif at higher discharge power.

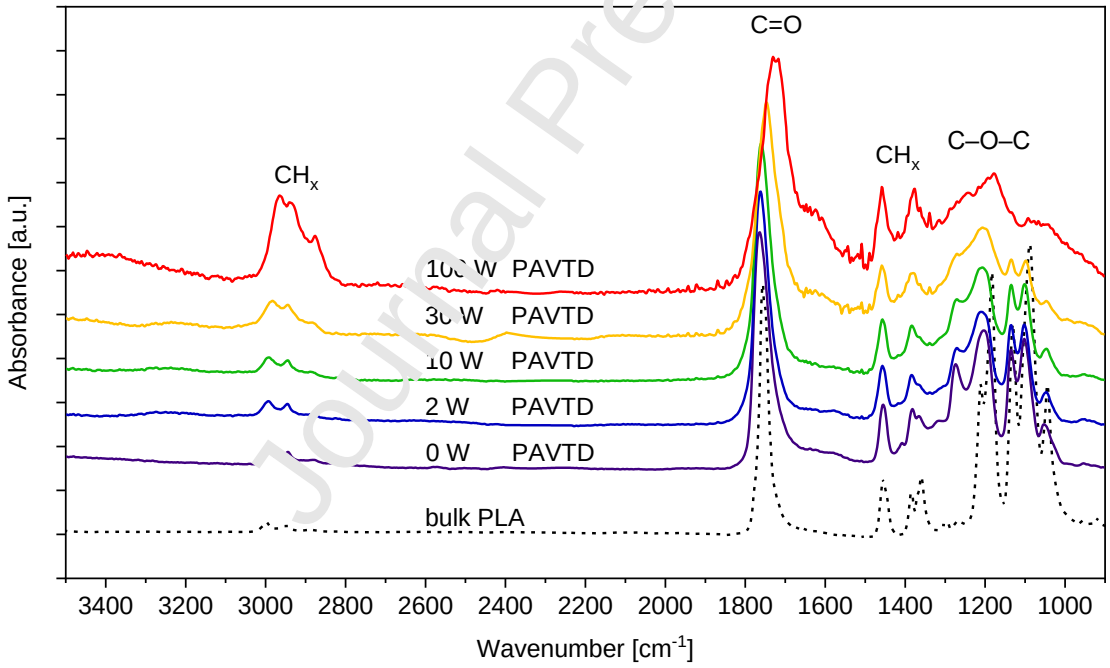

Figure 2 The FTIR spectra of PAVTD plasma polymerized thin films of PLA. The colour gradient distinguishes the discharge power during film preparation. The FTIR spectra are normalized to C=O vibration at ~ 1740 cm^{-1}. Tabulated FTIR-ATR spectrum of bulk PLA [51] is shown for comparison.

The alteration in the PLA chemical motif is further accompanied by changes in the macromolecular structure, manifested in the GPC measurements (Figure 3). Here, the red curve corresponds to the original PLA, showing the negatively skewed molar mass distribution that averages 4×10^3 $g\times mol^{-1}$. The curves of the plasma deposited films are shifted to the lower masses and have positive skewness. The phenomenon is closely related to the physical and chemical processes occurring during the deposition. Thermal decomposition of original PLA

macromolecules proceeds with a release of lower molar mass oligomers to the gas phase, with their subsequent deposition onto substrates. Such oligomers contribute to the molar mass distribution maximum ~350 g×mol^{-1} (~5 monomeric units). The activation by plasma leads to an additional bond cleavage with the formation of radicals that participate in recombination reactions during the diffusion over the substrate surface. The recombination processes are responsible for forming larger molar mass species, most probably branched, at the expense of the oligomers. Thus, the 350 g×mol^{-1} maximum decreases with the discharge power, whereas a broad, positively skewed shoulder develops.

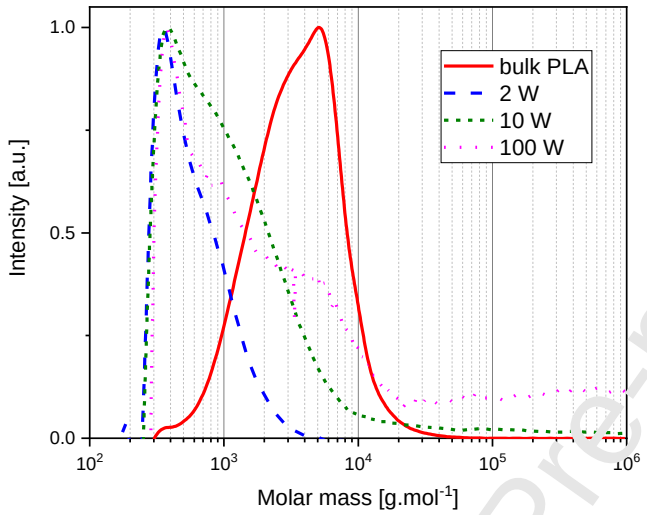

Figure 3 GPC molar mass distribution of the sol fraction of plasma polymerized PLA in dependence on the discharge power, scaled to the distribution maximum.

Another confirmation of the above findings can be found in the analysis of thermal stability tests, which showed a gradual loss of material with temperature, with the loss being slower for the high-power films (Figure 4). For example, the film prepared without plasma (0 W) showed about 20 % escape of material at 30 °C, whereas for the 100 W film, the same loss was observed at 160 °C. As was shown by GPC, plasma polymerized films contain a fraction of short uncross-linked chains. Their escape is driven by diffusion to the film surface, which can be hindered by entanglements with the cross-linked gel network. The slower material loss provides another indication of increased cross-linking in high-power films. Thus, the sol/gel fraction in plasma polymerized PLA thin films can be tuned by the discharge power, providing the basis for their use as controllable drug release platforms.

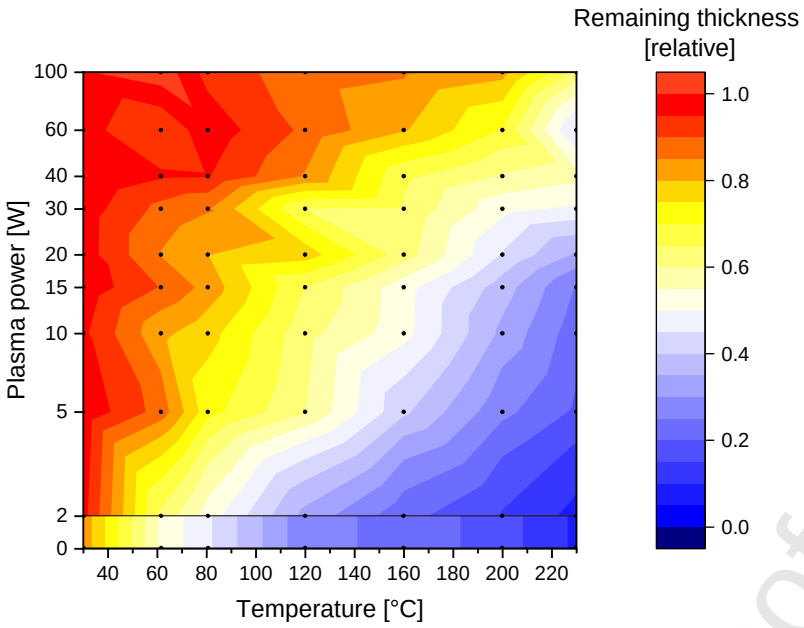

Figure 4 Thermal stability of plasma polymerized PLA in dependence on the plasma power during the film preparation. Relative remaining thickness corresponds to the ratio of thickness after and before the incubation. Black dots indicate the actual points of the measurement.

3.2 Stability in water – ex-situ ellipsometry

The GPC and thermal stability results are further supported by the *ex-situ* ellipsometry measurements of the film thickness performed before and after their incubation in water (Figure 5a). The inverse ratio of these thicknesses gives the gel volume fraction parameter, that is, the volume occupied by the gel with respect to the volume of all constituents (sol + gel) in the film. A complete dataset is summarized in a colour diagram, in which the colour palette codes the values of the gel fraction for specific combinations of the discharge power and the incubation time. The initial film thickness was 100 nm for all the powers investigated.

The films prepared with 0 W – 30 W power completely dissolve in water, although with different dissolution kinetics, which becomes delayed at higher power. The slower kinetics testifies that the films become enriched with larger macromolecules with an increase of the power, while the complete dissolution suggests that the infinite gel network has not been formed. The general trend agrees with the GPC and thermal stability measurements.

The point of gelation is reached above 30 W; here, the number of radical-bearing oligomers becomes sufficiently large to link themselves into a single macroscopic network. The dissolution kinetics of the soluble fraction follow the trend of slowing down with increased power; however, the complete dissolution is no longer reached. At 100 W, the films are highly cross-linked and do not dissolve in water, at least over the time range of one week.

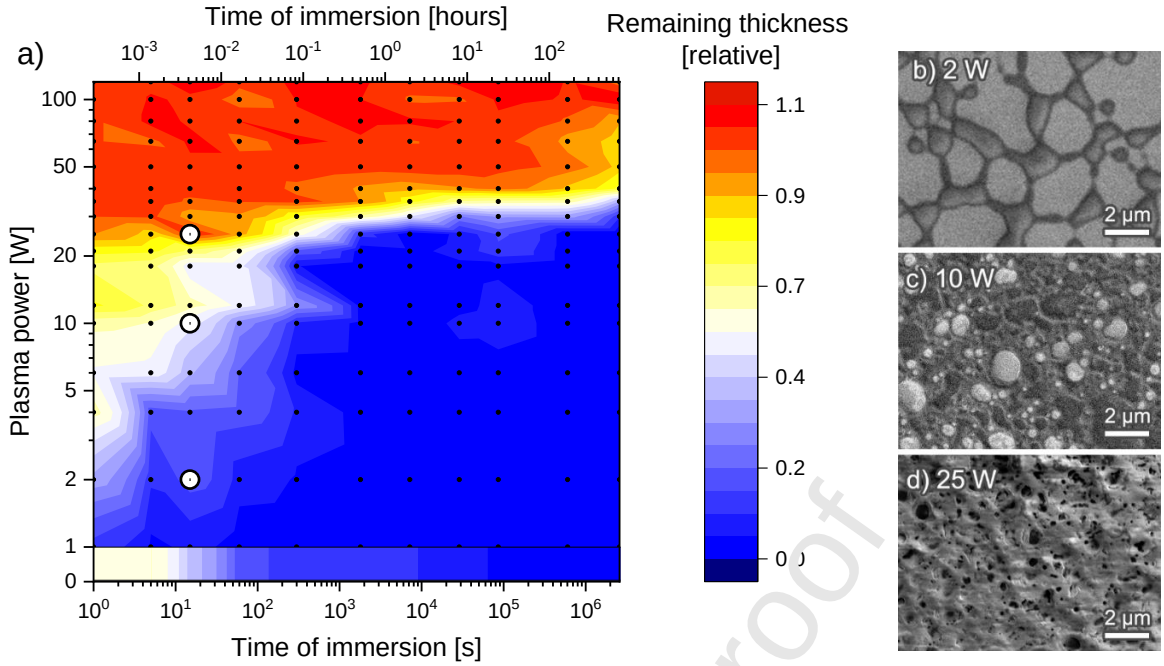

Figure 5 Effects of immersion of the films in water. a) The gel volume fraction in plasma polymerized PLA in dependence on the discharge power and the incubation time; the colour gradient determines the ratio of thickness after and before the incubation; black dots indicate the actual points of measurement. The outlined white points show where SEM images were obtained. b) SEM images of plasma polymerized PLA obtained after 15-second incubation in H_2O.

Figure 5b demonstrates the SEM images of the PLA thin films after being incubated in water for 15 seconds and dried afterwards. The 2 W film is the most unstable, showing a significant disintegration level and exposing the substrate between the interconnected islands of the film remnants. The film integrity is retained better at higher power, although clear signs of surface degradation are yet to be seen. The film prepared at 25 W is much more stable.

The thickness decay was analyzed quantitatively by fitting the experimental data to a multi-exponential polynomial:

$$T(\tau, P_i) = \sum a_{iP_i} e^{-\tau/t_i} \quad (1)$$

Here, $T(\tau, P_i)$ is the dry thickness of the film prepared at P_i discharge power at the time τ after the immersion, where $a_{i\,P_i}$ is the sol fraction of this film, which is dissolved with a characteristic time of t_i. It was necessary to use at least four terms in the polynomial to fit the data with acceptable accuracy, so the final expression is:

$$T(\tau, P_i) = a_{1\,P_i} e^{-\tau/t_1} + a_{2\,P_i} e^{-\tau/t_2} + a_{3\,P_i} e^{-\tau/t_3} + a_{4\,P_i} \quad (2)$$

The first term corresponds to the thickness decay in the first moments after the immersion to cover any changes at the timescale below the first measured data point (the shortest 1 s immersion time was possible). The second and third terms correspond to the delayed dissolution kinetics. The last term is responsible for the gel fraction that remains undissolved after the immersion. The characteristic time t_4 was set to ∞; therefore, the

fourth term is just a constant. As the model is applied to the relative thicknesses, the equation has to fulfil the normalization condition:

$$T(\tau = 0, P_i) = a_{1\,P_i} + a_{2\,P_i} + a_{3\,P_i} + a_{4\,P_i} = 1 \quad (3)$$

The experimental data with fitting curves corresponding to the discharge power of 6 W and 30 W are shown in Figure 6a, b, whereas the entire sets of a_i are given in Figure 6c. Table 1 summarizes the characteristic times obtained as a result of the fitting.

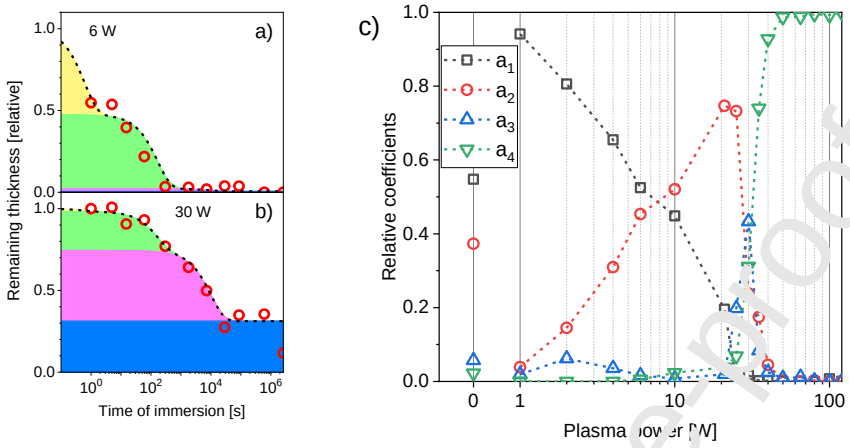

Figure 6 Thickness decay of the PLA plasma polymers after their immersion in water: a), b) film thickness in dependence on the immersion time for 6 and 30 W discharge power; open symbols are experimental data points; dashed lines are fits to Eq. 2; different colours guide the eye to distinguish regions with four dissolution kinetics: yellow – a_1, t_1 (fastest), green - a_2, t_2, magenta - a_3, t_3, blue - a_4, $t_4 = \infty$ (insoluble gel); c) a_i in dependence on the discharge power.

Table 1 Characteristic times ti obtained by fitting the experimental data to Eq. 2.

Characteristic time, s			
t_1	t_2	t_3	t_4
0.6	160	10100	∞

The low-power films are rich with smaller oligomers (a_1 is close to 1.0 for 1 W), which dissolve quickly upon immersion. The characteristic time t_1 is less than 1 s, so the experimental data are missing in this region. With increasing power, the a_1 fraction gradually decreases, whereas the a_2 and, to a lesser extent, the a_3 and a_4 fractions increase, confirming the enhancement of the re-polymerization processes and the formation of larger macromolecules. For the most part, such macromolecules are not part of the infinite gel network, and they still dissolve, although with longer characteristic times of $t_2 \sim 10^2$ s and $t_3 \sim 10^4$ s. All the soluble fractions eventually disappear at about 30 W, while the insoluble gel fraction a_4 becomes dominating. Thus, the model supports the above findings of the onset of gelation at about 30 W. It also provides additional insight into the dissolution kinetics at low power, pointing to the existence of three characteristic times that span over a broad time scale of 10^{-1} - 10^4 s.

3.3 Stability in water – in-situ ellipsometry

The more demanding ellipsometry measurements were performed *in-situ* using the liquid cell to analyze both the dissolution and swelling of the PLA plasma polymers when in contact with water (Figure 7). The relative thickness was calculated as the ratio of the film thickness at a given incubation time to the initial dry thickness. Different colours code the volume fraction of water absorbed in the film and the polymer fraction as detected by the fitting of the ellipsometry data.

For the low-power films, the interaction with water starts with an abrupt thickness decrease immediately after the immersion. Note that the first data point is acquired after the fast dissolution of the light oligomer fraction has already occurred, as shown above. The initial thickness decrease is followed by a gradual increase until a maximal value is reached. At the final stage, the thickness decreases again and approaches the equilibrium level. With increasing power, the maximal thickness is observed at longer incubation time. The high-power films are much more stable, showing a minor initial thickness decrease, little swelling, and a modest final thickness decrease (or none of the above for the 100 W film).

Such a non-trivial thickness evolution of plasma polymerized PLA is a consequence of two concurring processes: the release of the sol fraction, which contributes to a decrease in the film thickness, and swelling of the gel fraction, which leads to an increase of the film thickness. The free volume in the swollen films becomes occupied by absorbed water molecules. The dissolution kinetics depends on the average molar mass of the released species and the average molar mass of chains between cross-links. The kinetics of swelling is determined by the finite extensibility of network chains and by adhesion constraints [42,52,53]. All these parameters are simultaneously influenced by the discharge power, which determines the overall thickness evolution. With the increasing power, the average molar mass of the sol increases while chain length between cross-links decreases, thus providing a macromolecular sieve of finer scale. Therefore, the dissolution is retarded and extended in time. At the same time, shorter chains between cross-links have limited extensibility, thus reducing the swelling effects, and the remaining swollen network is characterized by a smaller free volume.

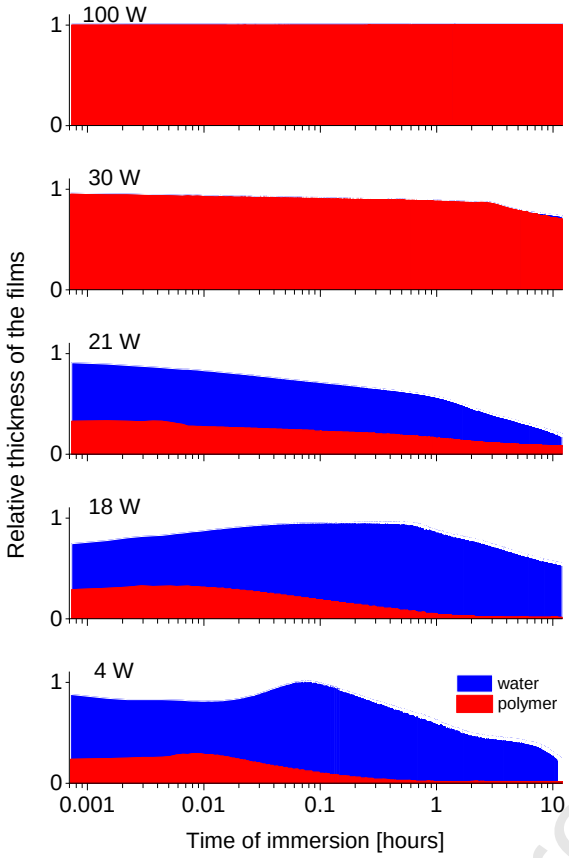

Figure 7 Relative thickness of plasma polymerized PLA in dependence on the discharge power and the incubation time as measured by *in-situ* liquid-cell ellipsometry; red and blue colours designate the polymer and absorbed water fractions.

3.4 Stability in water – Hydrolysis

Hydrolysis of conventional PLA is known to comprise the backbone scission and the release of monomeric lactic acid (LA) [54,55] as demonstrated in Scheme 1. Therefore, LC-MS was engaged to study the LA release kinetics from plasma polymerized PLA during their hydrolysis. Figure 8 shows the results in dependence on the discharge power. The films deposited at low power are the most vulnerable to hydrolysis, demonstrating an almost immediate release of LA and yielding the maximal LA concentration after four incubation days. As the discharge power increases, the LA concentration is reduced, which coincides with reducing the sol fraction. However, as was shown by ellipsometry, the polymer dissolution kinetics is faster, with the highest characteristic time being ~ 10^4 s (about 2.5 hours). Thus, the hydrolysis can be attributed mainly to the degradation of soluble PLA macromolecules when they are already in the liquid phase. The gel network hydrolysis is of secondary importance because the molecular chains between the cross-links are less accessible and better withstand attacks from water molecules. At the power >50 W, the LA concentration decreases below the LC-MS detection limit, reflecting a highly-crosslinked character of these plasma polymers.

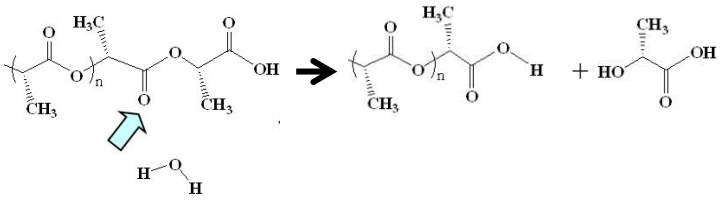

Scheme 1 Reaction scheme of PLA hydrolysis.

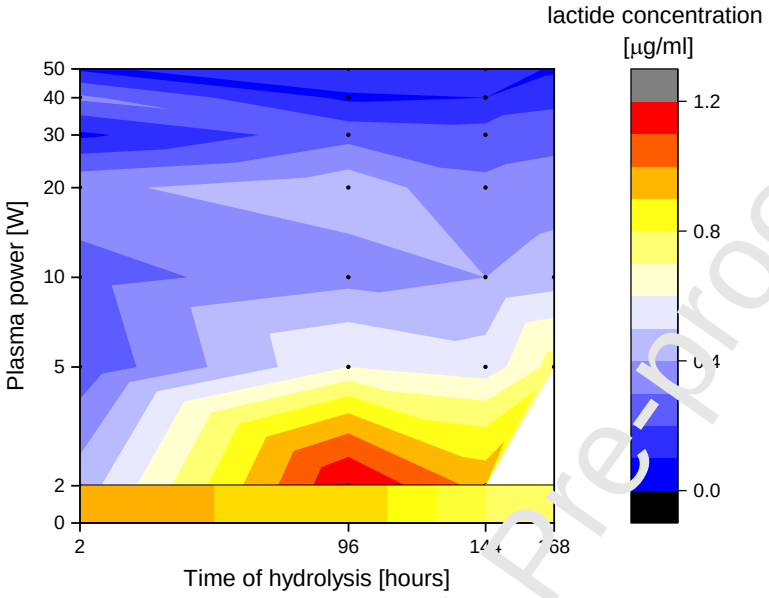

Figure 8 LC-MS concentration of lactic acid released due to hydrolysis of plasma polymerized PLA in dependence on the discharge power and H_2O incubation time. Black dots indicate the actual points of the measurement.

3.5 Biomolecule release

Since molecule ability to diffuse within a polymer matrix strongly depends on the available free volume, plasma polymerized PLA can be tailored to the specific needs of controllable drug release. The feature was demonstrated using nisin, an antibacterial peptide of about 3300 g×mol^{-1} molar mass. Layers of nisin/PVA mixtures with 45 nm thickness were overcoated by 70 nm thick plasma polymerized PLA coatings and then subjected to incubation in water. The concentration of nisin in the solution above the sample surface was determined at different time intervals by HPLC/UV, and the resultant kinetics is shown in Figure 9 in dependence on the discharge power.

It is noteworthy that the nisin release shows two maxima belonging to low- and high-power films, both maxima propagating in the direction from smaller power/shorter time toward their higher values. For the low-power films, the release maximum is readily explained within the above paradigm of polymer-free volume and film dissolution. In this case, the polymer topology implies the existence of free volume at different length scales. Inherent to all polymers, the free space exists at the molecular length scale and is associated with voids between the macromolecular segments. On the other hand, the soluble phase dissolution leaves pores with a dynamically changing size that reaches the micron length scale (Figure 5).

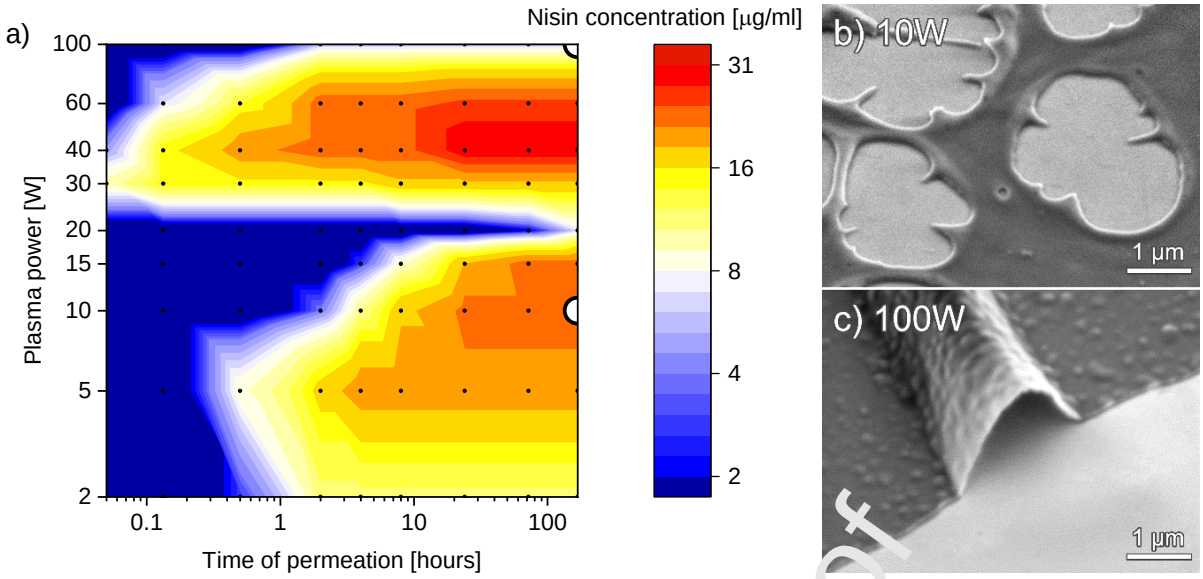

Figure 9 Release of nisin form the films. a) Kinetics of the cumulative nisin permeation through thin films of plasma polymerized PLA in dependence on the discharge power and the incubation time. The black dots indicate the actual points of the measurement. The outlined white points correspond to SEM images shown in b) and c).

It takes nisin macromolecules time to diffuse through the film, which simultaneously undergoes dissolution, and the first signs of nisin manifest themselves in solution after about 10 min of incubation. Considering the relatively large nisin molecular size of several nanometers [56,57], it can be suggested that the diffusion proceeds with less probability via the molecular scale-sized free volume but rather via micron-sized porous channels created as a result of the polymer dissolution. With increasing power, the film's pores become less abundant, and their size decreases, so the onset of the nisin release can be observed at longer incubation times. At the point of gelation, at which an infinite polymer network is formed, the film remains continuous, and the micron-sized pores are no longer available for diffusion, preventing the nisin permeation and keeping its concentration in the solution below the detection limit. A similar effect of cross-linking and the plasma pretreatment was confirmed earlier for PVA matrices used as carriers for nisin [58].

Markedly, a further increase of the discharge power results in the films becoming permeable to nisin again. However, unlike the low-power films, the permeation kinetics is fast, and nisin is detected immediately after the immersion into water. Since the cross-link density is very high and the free volume is low, fast nisin release should be associated with macroscopic scale phenomena and attributed to morphological instabilities occurring in these films.

SEM images were acquired to demonstrate these effects on the PLA thin films deposited at different discharge power over the nisin/PVA coatings. The 10 W sample shows strong signs of degradation, propagating from sub-micron-sized pores for shorter incubation (Figure 5) to micron-sized holes for the 7-day incubation (Figure 9b). In contrast to the holes, the film deposited at 100 W exhibits micron-sized folds, which point to buckling instabilities being accompanied by delamination (Figure 9c). Buckling belongs to well-known morphological instabilities of soft matter, polymers in particular, and is associated with the accumulation of compressive stress in the film [59,60]. Polymer films adhering to rigid substrate withstand the build-up of stress

until a critical point is reached, at which the stress overcomes the adhesion and the film relaxes, increasing its volume by buckling. Plasma polymer films, including those studied here, are deposited far from equilibrium conditions, and the accumulation of compressive stress in them is typical. At high power, the stress is high and can be relaxed by a subtle perturbation. In the case of plasma polymerized PLA, we attribute the perturbation effects qualitatively to water molecules that penetrate the hydrophilic polymer matrix and exert an osmotic force on the network chains, forcing them to extend. The timescale of this process shall be at least comparable to the dynamics of the stability of the films in water, as described earlier, or faster [61]. Since the films adhere to substrates, swelling stress develops, which contributes to the compressive stress. The adhesion still prevails for the low-power films, and the films expand only in the direction normal to the substrate (swelling) but without delamination. In the high-power films, the compressive stress is high so that the addition of the swelling stress exceeds the instability threshold, and the film collapses by buckling and delamination.

Generally, the buckling effect can be considered unwanted because it violates the film/substrate system integrity. However, in the drug release agenda, buckling can be regarded as an asset rather than a drawback, opening the way to switching the kinetics to a fast release. Indeed, nisin escape starts and finishes faster for the high-power films, which we attribute to nisin diffusion through the macroscopic buckling channels created in these films. Interestingly, no buckling was observed for the same films deposited onto glass substrate without a nisin coating, which evidences stronger adhesion forces between the plasma polymer and glass than between physically adsorbed nisin/PVA coating and glass.

3.6 Antibacterial effect

The observed peculiarities of the nisin release are pronounced in the bactericidal activity of the prepared samples. Differently cross-linked nisin-loaded PLA samples were incubated in water for several days. After defined periods, the solution's aliquots were taken and placed onto agar disks seeded with bacteria. The diameters of inhibition zones (including the diameter of the well) were recorded (Table 2).

Table 2 Inhibition zones of the nisin/PLA samples obtained against *M. luteus* after several day incubation in water.

Sample	Inhibition zone diameter [mm]		
	1-day incubation	2-day incubation	10-day incubation
PLA 0W	9	11	9
PLA 5W	9	10	12
PLA 20W	12	10	8

Although the results do not agree precisely with the nisin permeation tests of Figure 9 obtained for different series of the samples, they follow the general trend. The uncross-linked PLA film (0 W) exhibits a local bactericidal maximum after 2 days of incubation, and then the bactericidal activity diminishes. The inhibition zones ultimately observed for the solutions from all the samples are similar, making this way also a rough control of the retention of nisin activity after exposure to plasma, similarly to [47]. For the weakly cross-linked film (5 W), a gradual increase of the antibacterial effect is observed, attributed to the delayed nisin release and evidencing that the maximal release has yet not been achieved even after the 10-day incubation. By contrast, for

the stronger cross-linked film (20 W), the highest bactericidal activity is observed after the first day of incubation, and then it subsides to zero inhibition zone, being consistent with the fast nisin release from this type of coatings.

4. Conclusions

Thin films of cross-linked polyesters can be prepared by Plasma-Assisted Vapor Thermal Deposition of PLA with the chemical composition and cross-link density tuned by the discharge power. The plasma activates the oligomers released due to the thermal evaporation of PLA and assists in forming radical-bearing species. Plasma-activated oligomers deposit on substrates and participate in recombination reactions, thereby providing cross-links. The low power results in weakly cross-linked films, closely matching the chemical motif of PLA. The molar mass distribution shows a maximum at ~350 $g \times mol^{-1}$ and skews to larger species. The skewness enhances with the power, reflecting the intensification of the re-polymerization processes and the formation of large, branched macromolecules. At about 30 W power, the gel point is reached, at which an infinite macromolecular network appears. Further increase of the discharge power leads to highly cross-linked films with the impaired retention of the PLA character.

The films interact with water by swelling and dissolution, with the sol/gel ratio also controlled by the discharge power. The dissolution obeys a multi-exponential decay, and the characteristic time spans over a broad scale of $10^{-1} - 10^{4}$ seconds. The soluble phase hydrolyzes when in solution, with the characteristic hydrolysis time reaching days. Lactic acid was found to be a product of such hydrolysis, evidencing the film's biodegradability. During the dissolution, the low-power films (prepared below the gel point) disintegrate, exposing micrometre-sized pores. The high-power films retain their integrity yet showing buckling instabilities and delamination due to the enhanced compressive stress. Thus, the PLA plasma polymers can be used as sacrificial layers for controlled drug release. The idea was implemented by depositing plasma polymerized PLA over layers of nisin, an antibacterial peptide. The low-power PLA films ensured the nisin permeation through micron-sized pores, resulting in a delayed drug release at a time scale of hours or days. The high-power PLA films demonstrated the nisin release via the buckling instabilities, which provided more efficient channels for the drug escape at a time scale of minutes. The PLA plasma polymers with nisin underlayers demonstrated bactericidal activity against *Micrococcus luteus*, and the efficiency correlated with the morphological topology of the plasma polymers. Thus, the developed films are very perspective as platforms for tissue-contacting devices with tunable drug release and therapeutic effect.

5. Acknowledgements

The research was chiefly funded by the Czech Science Foundation through the grant GA17-10813S. The Charles University's financial support via the student grant SVV 260 579/2021 and support from the Ministry of Industry and Trade of the Czech Republic via the project TRIO FV10400 are also acknowledged.

6. References

[1] S. Yoshida, K. Hagiwara, T. Hasebe, A. Hotta, Surface modification of polymers by plasma treatments for the enhancement of biocompatibility and controlled drug release, Surf. Coatings Technol. 233 (2013) 99–107. https://doi.org/10.1016/j.surfcoat.2013.02.042.

[2] P. Stloukal, I. Novák, M. Mičušík, M. Procházka, P. Kucharczyk, I. Chodák, M. Lehocký, V. Sedlařík, Effect of plasma

treatment on the release kinetics of a chemotherapy drug from biodegradable polyester films and polyester urethane films, Int. J. Polym. Mater. Polym. Biomater. 67 (2018) 161–173. https://doi.org/10.1080/00914037.2017.1309543.

[3] D.G. Petlin, S.I. Tverdokhlebov, Y.G. Anissimov, Plasma treatment as an efficient tool for controlled drug release from polymeric materials: A review, J. Control. Release. 266 (2017) 57–74. https://doi.org/10.1016/j.jconrel.2017.09.023.

[4] N. Kamaly, B. Yameen, J. Wu, O.C. Farokhzad, Degradable Controlled-Release Polymers and Polymeric Nanoparticles: Mechanisms of Controlling Drug Release, Chem. Rev. 116 (2016) 2602–2663. https://doi.org/10.1021/acs.chemrev.5b00346.

[5] M. Kanamala, W.R. Wilson, M. Yang, B.D. Palmer, Z. Wu, Mechanisms and biomaterials in pH-responsive tumour targeted drug delivery: A review, Biomaterials. 85 (2016) 152–167. https://doi.org/10.1016/j.biomaterials.2016.01.061.

[6] B. Tyler, D. Gullotti, A. Mangraviti, T. Utsuki, H. Brem, Polylactic acid (PLA) controlled delivery carriers for biomedical applications, Adv. Drug Deliv. Rev. 107 (2016) 163–175. https://doi.org/10.1016/j.addr.2016.06.018.

[7] R. Jalil, J.R. Nixon, Biodegradable poly(lactic acid) and poly(lactide-co-glycolide) microcapsules: problems associated with preparative techniques and release properties, J. Microencapsul. 7 (1990) 297–325. https://doi.org/10.3109/02652049009021842.

[8] F. Rancan, D. Papakostas, S. Hadam, S. Hackbarth, T. Delair, C. Primard, B. Verrier, W. Sterry, U. Blume-Peytavi, A. Vogt, Investigation of Polylactic Acid (PLA) Nanoparticles as Drug Delivery Systems for Local Dermatotherapy, Pharm. Res. 26 (2009) 2027–2036. https://doi.org/10.1007/s11095-009-9919-x.

[9] K. Hamad, M. Kaseem, H.W. Yang, F. Deri, Y.G. Ko, Properties and medical applications of polylactic acid: A review, Express Polym. Lett. 9 (2015) 435–455. https://doi.org/10.3144/expresspolymlett.2015.42.

[10] D. da Silva, M. Kaduri, M. Poley, O. Adir, N. Krinsky, J. Shainsky-Roitman, A. Schroeder, Biocompatibility, biodegradation and excretion of polylactic acid (PLA) in medical implants and theranostic systems, Chem. Eng. J. 340 (2018) 9–14. https://doi.org/10.1016/j.cej.2018.01.010.

[11] F. Zou, X. Sun, X. Wang, Elastic, hydrophilic and biodegradable poly (1, 8-octanediol-co-citric acid)/polylactic acid nanofibrous membranes for potential wound dressing applications, Polym. Degrad. Stab. 166 (2019) 163–173. https://doi.org/10.1016/j.polymdegradstab.2019.05.014.

[12] R.P. Pawar, S.U. Tekale, S.U. Shisodia, J.T. Totre, A.J. Domb, Biomedical applications of poly(lactic acid), Rec. Pat. Regen. Med. 4 (2014) 40–51. https://doi.org/10.2174/22103965044666140402235024.

[13] M. Turalija, S. Bischof, A. Budimir, S. Gaan, Antimicrobial PLA films from environment friendly additives, Compos. Part B Eng. 102 (2016) 94–99. https://doi.org/10.1016/j.compositesb.2016.07.017.

[14] T. Casalini, F. Rossi, A. Castrovinci, G. Perale, A Perspective on Polylactic Acid-Based Polymers Use for Nanoparticles Synthesis and Applications, Front. Bioeng. Biotechnol. 7 (2019). https://doi.org/10.3389/fbioe.2019.00259.

[15] V. DeStefano, S. Khan, A. Tabada, Applications of PLA in modern medicine, Eng. Regen. 1 (2020) 76–87. https://doi.org/10.1016/j.engreg.2020.08.002.

[16] E. Stoleru, T. Zaharescu, E.C. Hitruc, A. Vesel, E.G. Ioanid, A. Coroaba, A. Safrany, G. Pricope, M. Lungu, C. Schick, C. Vasile, Lactoferrin-immobilized surfaces onto functionalized PLA assisted by the gamma-rays and nitrogen plasma to create materials with multifunctional properties, ACS Appl. Mater. Interfaces. 8 (2016) 31902–31915. https://doi.org/10.1021/acsami.6b09069.

[17] P. Kucharczyk, E. Hnatkova, Z. Dvorak, V. Sedlarik, Novel aspects of the degradation process of PLA based bulky samples under conditions of high partial pressure of water vapour, Polym. Degrad. Stab. 98 (2013) 150–157. https://doi.org/10.1016/j.polymdegradstab.2012.10.016.

[18] H. Tsuji, H. Muramatsu, Blends of aliphatic polyesters: V non-enzymatic and enzymatic hydrolysis of blends from hydrophobic poly(l-lactide) and hydrophilic poly(vinyl alcohol), Polym. Degrad. Stab. 71 (2001) 403–413. https://doi.org/10.1016/S0141-3910(00)00192-0.

[19] H. Tsuji, S. Miyauchi, Poly(l-lactide): VI Effects of crystallinity on enzymatic hydrolysis of poly(l-lactide) without free amorphous region, Polym. Degrad. Stab. 71 (2001) 415–424. https://doi.org/10.1016/S0141-3910(00)00191-9.

[20] H. Tsuji, Y. Echizen, Y. Nishimura, Enzymatic Degradation of Poly(l-Lactic Acid): Effects of UV Irradiation, J. Polym. Environ. 14 (2006) 239–248. https://doi.org/10.1007/s10924-006-0023-6.

[21] Y. Qi, H.-L. Ma, Z.-H. Du, B. Yang, J. Wu, R. Wang, X.-Q. Zhang, Hydrophilic and Antibacterial Modification of Poly(lactic

acid) Films by γ-ray Irradiation, ACS Omega. 4 (2019) 21439–21445. https://doi.org/10.1021/acsomega.9b03132.

[22] H.S. Yoo, T.G. Kim, T.G. Park, Surface-functionalized electrospun nanofibers for tissue engineering and drug delivery, Adv. Drug Deliv. Rev. 61 (2009) 1033–1042. https://doi.org/10.1016/j.addr.2009.07.007.

[23] S. Simovic, D. Losic, K. Vasilev, Controlled drug release from porous materials by plasma polymer deposition, Chem. Commun. 46 (2010) 1317. https://doi.org/10.1039/b919840g.

[24] P. Pleskunov, D. Nikitin, R. Tafiichuk, I. Khalakhan, Z. Kolská, A. Choukourov, Nanophase-separated poly(acrylic acid)/poly(ethylene oxide) plasma polymers for the spatially localized attachment of biomolecules, Plasma Process. Polym. (2020) e1900220. https://doi.org/10.1002/ppap.201900220.

[25] M.J. Garcia-Fernandez, L. Martinez-Calvo, J.-C. Ruiz, M.R. Wertheimer, A. Concheiro, C. Alvarez-Lorenzo, Loading and Release of Drugs from Oxygen-rich Plasma Polymer Coatings, Plasma Process. Polym. 9 (2012) 540–549. https://doi.org/10.1002/ppap.201100192.

[26] C. Amorosi, V. Ball, J. Bour, P. Bertani, V. Toniazzo, D. Ruch, L. Averous, M. Michel, One step preparation of plasma based polymer films for drug release, Mater. Sci. Eng. C. 32 (2012) 2103–2108. https://doi.org/10.1016/j.msec.2012.05.045.

[27] F. Truica-Marasescu, M.R. Wertheimer, Nitrogen-Rich Plasma-Polymer Films for Biomedical Applications, Plasma Process. Polym. 5 (2008) 44–57. https://doi.org/10.1002/ppap.200700077.

[28] P. Solař, O. Polonskyi, A. Choukourov, A. Artemenko, J. Hanuš, H. Biederman, D. Slavínská, Nanostructured thin films prepared from cluster beams, Surf. Coatings Technol. 205 (2011) S42–S47. https://doi.org/10.1016/j.surfcoat.2011.01.059.

[29] D. Shi, J. Lian, P. He, L.M. Wang, F. Xiao, L. Yang, M.J. Schulz, D.B. Mast, Plasma coating of carbon nanofibers for enhanced dispersion and interfacial bonding in polymer composites, Appl. Phys. Lett. 83 (2003) 5301–5303. https://doi.org/10.1063/1.1636521.

[30] P. Favia, R. D'Agostino, Plasma treatments and plasma deposition of polymers for biomedical applications, Surf. Coatings Technol. 98 (1998) 1102–1106. https://doi.org/10.1016/S0257-8972(97)00285-5.

[31] F. Denes, Macromolecular plasma-chemistry: an emerging field of polymer science, Prog. Polym. Sci. 29 (2004) 815–885. https://doi.org/10.1016/j.progpolymsci.2004.05.001.

[32] P. Pleskunov, D. Nikitin, R. Tafiichuk, A. Shelemin, J. Hanuš, I. Khalakhan, A. Choukourov, Carboxyl-Functionalized Nanoparticles Produced by Pulsed Plasma Polymerization of Acrylic Acid, J. Phys. Chem. B. 122 (2018) 4187–4194. https://doi.org/10.1021/acs.jpcb.8b01648.

[33] P. Pleskunov, D. Nikitin, R. Tafiichuk, A. Shelemin, J. Hanuš, J. Kousal, Z. Krtouš, I. Khalakhan, P. Kúš, T. Nasu, T. Nagahama, C. Funaki, H. Sato, M. Sawek, A. Schoenhals, A. Choukourov, Plasma Polymerization of Acrylic Acid for the Tunable Synthesis of Glassy and Carboxylated Nanoparticles, J. Phys. Chem. B. 124 (2020) 668–678. https://doi.org/10.1021/acs.jpcb.9b08960.

[34] S. Ligot, F. Renaux, L. Denis, D. Cossement, N. Nuns, P. Dubois, R. Snyders, Experimental study of the plasma polymerization of ethyl lactate, Plasma Process. Polym. 10 (2013) 999–1009. https://doi.org/10.1002/ppap.201300025.

[35] J. Friedrich, Mechanisms of plasma polymerization - Reviewed from a chemical point of view, Plasma Process. Polym. 8 (2011) 783–802. https://doi.org/10.1002/ppap.201100038.

[36] V. Kumar, J. Pulpytel, H. Rauscher, I. Mannelli, F. Rossi, F. Arefi-khonsari, Fluorocarbon Coatings Via Plasma Enhanced Chemical Vapor Deposition of 1H , 1H , 2H , 2H- perfluorodecyl Acrylate - 2 , Morphology , Wettability and Antifouling Characterization a, Plasma Process. Polym. 7 (2010) 926–938. https://doi.org/10.1002/ppap.201000038.

[37] R. Gristina, E.D. Aloia, G.S. Senesi, A. Milella, M. Nardulli, E. Sardella, P. Favia, R. Agostino, Increasing Cell Adhesion on Plasma Deposited Fluorocarbon Coatings by Changing the Surface Topography, J. Biomed. Mater. Res. Part B Appl. Biomater. 88B (2008) 139–149. https://doi.org/10.1002/jbm.b.31160.

[38] M. Ji, A. Jagodar, E. Kovacevic, L. Benyahia, F. Poncin-epaillard, I. Mol, Characterization of functionalized coatings prepared from pulsed plasma polymerization, Mater. Chem. Phys. 267 (2021) 124621. https://doi.org/10.1016/j.matchemphys.2021.124621.

[39] A. Choukourov, J. Hanuš, J. Kousal, A. Grinevich, Y. Pihosh, D. Slavínská, H. Biederman, Thin polymer films from polyimide vacuum thermal degradation with and without a glow discharge, Vacuum. 80 (2006) 923–929. https://doi.org/10.1016/j.vacuum.2005.12.012.

[40] A. Choukourov, I. Gordeev, O. Polonskyi, A. Artemenko, L. Hanyková, I. Krakovský, O. Kylián, D. Slavínská, H. Biederman, Polyethylene (ethylene oxide)-like plasma polymers produced by plasma-assisted vacuum evaporation, Plasma Process. Polym. 7 (2010) 445–458. https://doi.org/10.1002/ppap.200900153.

[41] A. Choukourov, I. Gordeev, D. Arzhakov, A. Artemenko, J. Kousal, O. Kylián, D. Slavínská, H. Biederman, Does cross-link density of PEO-like plasma polymers influence their resistance to adsorption of fibrinogen?, Plasma Process. Polym. 9 (2012) 48–58. https://doi.org/10.1002/ppap.201100122.

[42] K. Dušek, A. Choukourov, M. Dušková-Smrčková, H. Biederman, Constrained Swelling of Polymer Networks: Characterization of Vapor-Deposited Cross-Linked Polymer Thin Films, Macromolecules. 47 (2014) 4417–4427. https://doi.org/10.1021/ma5006217.

[43] D. Margarone, I.J. Kim, J. Psikal, J. Kaufman, T. Mocek, I.W. Choi, L. Stolcova, J. Proska, A. Choukourov, I. Melnichuk, O. Klimo, J. Limpouch, J.H. Sung, S.K. Lee, G. Korn, T.M. Jeong, Laser-driven high-energy proton beam with homogeneous spatial profile from a nanosphere target, Phys. Rev. Spec. Top. - Accel. Beams. 18 (2015) 071304. https://doi.org/10.1103/PhysRevSTAB.18.071304.

[44] A. Choukourov, I. Gordeev, J. Ponti, C. Uboldi, I. Melnichuk, M. Vaidulych, J. Kousal, D. Nikitin, L. Hanyková, I. Krakovský, D. Slavínská, H. Biederman, Microphase-Separated PE/PEO Thin Films Prepared by Plasma-Assisted Vapor Phase Deposition, ACS Appl. Mater. Interfaces. 8 (2016) 8201–8212. https://doi.org/10.1021/acsami.5b12382.

[45] A. Choukourov, P. Pleskunov, D. Nikitin, R. Tafiichuk, A. Shelemin, J. Hanuš, J. Májek, M. Unger, A. Roy, A. Ryabov, Plasma-assisted growth of polyethylene fractal nano-islands on polyethylene oxide films: Impact of film confinement and glassy dynamics on fractal morphologies, Appl. Surf. Sci. 489 (2019) 55–65. https://doi.org/10.1016/j.apsusc.2019.05.287.

[46] J. Kousal, Z. Krtouš, Z. Kolářová Rašková, J. Sedlaříková, J. Schäfer, L. Kučerová, A. Shelemin, P. Solař, A. Hurajová, H. Biederman, M. Lehocký, Degradable plasma polymer films with tailored hydrolysis behavior, Vacuum. 173 (2020). https://doi.org/10.1016/j.vacuum.2019.109062.

[47] J. Kousal, J. Sedlaríková, Z. Kolářová-Rašková, Z. Krtouš, L. Kucerová, A. Hurajová, M. Vaidulych, J. Hanuš, M. Lehockỳ, Degradable poly(ethylene oxide)-like plasma polymer films used for the controlled release of nisin, Polymers (Basel). 12 (2020). https://doi.org/10.3390/POLYM12061263.

[48] Z. Krtouš, L. Hanyková, I. Krakovský, D. Nikitin, P. Pleskunov, O. Kylián, J. Sedlaříková, J. Kousal, Structure of plasma (Re)polymerized polylactic acid films fabricated by plasma-assisted vapour thermal deposition, Materials (Basel). 14 (2021) 1–12. https://doi.org/10.3390/ma14020453.

[49] A. Copinet, C. Bertrand, S. Govindin, V. Coma, Y. Couturier, Effects of ultraviolet light (315 nm), temperature and relative humidity on the degradation of polylactic acid plastic films, Chemosphere. 55 (2004) 763–773. https://doi.org/10.1016/j.chemosphere.2003.11.038.

[50] H.-Y. Mi, M.R. Salick, X. Jing, B.R. Jacques, W.C. Crone, X.-F. Peng, L.-S. Turng, Characterization of thermoplastic polyurethane/polylactic acid (TPU/PLA) tissue engineering scaffolds fabricated by microcellular injection molding, Mater. Sci. Eng. C. 33 (2013) 4767–4776. https://doi.org/10.1016/j.msec.2013.07.037.

[51] J. Kousal, Z. Kolářová Rašková, J. Sedlaříková, P. Stloukal, P. Solař, Z. Krtouš, A. Choukourov, V. Sedlařík, M. Lehocký, Plasma polymers with controlled degradation behaviour, NANOCON 2017 - Conf. Proceedings, 9th Int. Conf. Nanomater. - Res. Appl. 2017-Octob (2018) 461–466.

[52] R. Toomey, D. Freidank, J. Rühe, Swelling Behavior of Thin, Surface-Attached Polymer Networks, Macromolecules. 37 (2004) 882–887. https://doi.org/10.1021/ma034737v.

[53] A. Vidyasagar, J. Majewski, R. Toomey, Temperature Induced Volume-Phase Transitions in Surface-Tethered Poly(N -isopropylacrylamide) Networks, Macromolecules. 41 (2008) 919–924. https://doi.org/10.1021/ma071438n.

[54] P. Stloukal, A. Kalendova, H. Mattausch, S. Laske, C. Holzer, M. Koutny, The influence of a hydrolysis-inhibiting additive on the degradation and biodegradation of PLA and its nanocomposites, Polym. Test. 41 (2015) 124–132. https://doi.org/10.1016/j.polymertesting.2014.10.015.

[55] P. Stloukal, G. Jandikova, M. Koutny, V. Sedlařík, Carbodiimide additive to control hydrolytic stability and biodegradability of PLA, Polym. Test. 54 (2016) 19–28. https://doi.org/10.1016/j.polymertesting.2016.06.007.

[56] R. Weishaupt, L. Heuberger, G. Siqueira, B. Gutt, T. Zimmermann, K. Maniura-Weber, S. Salentinig, G. Faccio, Enhanced

Antimicrobial Activity and Structural Transitions of a Nanofibrillated Cellulose–Nisin Biocomposite Suspension, ACS Appl. Mater. Interfaces. 10 (2018) 20170–20181. https://doi.org/10.1021/acsami.8b04470.

[57] S.-T.D. Hsu, E. Breukink, E. Tischenko, M.A.G. Lutters, B. de Kruijff, R. Kaptein, A.M.J.J. Bonvin, N.A.J. van Nuland, The nisin–lipid II complex reveals a pyrophosphate cage that provides a blueprint for novel antibiotics, Nat. Struct. Mol. Biol. 11 (2004) 963–967. https://doi.org/10.1038/nsmb830.

[58] Z. Kolarova Raskova, P. Stahel, J. Sedlarikova, L. Musilova, M. Stupavska, M. Lehocky, The effect of plasma pretreatment and cross-linking degree on the physical and antimicrobial properties of nisin-coated PVA films, Materials (Basel). 11 (2018). https://doi.org/10.3390/ma11081451.

[59] L.F. Francis, A. V. Mccormick, D.M. Vaessen, J.A. Payne, Development and measurement of stress in polymer coatings, J. Mater. Sci. 37 (2002) 4717–4731. https://doi.org/10.1023/A:1020886802632.

[60] H. Mei, R. Huang, J.Y. Chung, C.M. Stafford, H.-H. Yu, Buckling modes of elastic thin films on elastic substrates, Appl. Phys. Lett. 90 (2007) 151902. https://doi.org/10.1063/1.2720759.

[61] C. Liu, M.C. Lopes, S.A. Pihan, D. Fell, M. Sokuler, H.J. Butt, G.K. Auernhammer, E. Bonaccurso, Water diffusion in polymer nano-films measured with microcantilevers, Sensors Actuators, B Chem. 160 (2011) 32–38. https://doi.org/10.1016/j.snb.2011.07.007.

CRediT author statement

Zdeněk Krtouš: Methodology, Investigation, Formal analysis, Visualization, Writing - Review & Editing

Jaroslav Kousal: Conceptualization, Methodology, Investigation, Visualization, Writing - Review & Editing, Supervision, Project administration, Funding acquisition

Jana Sedlaříková: Methodology, Investigation, Resources, Writing - Review & Editing

Zuzana Kolářová Rašková: Conceptualization, Methodology, Investigation, Writing - Review & Editing

Liliana Kučerová: Investigation

Ivan Krakovský: Investigation

Jaromír Kučera: Resources

Suren Ali-Ogly: Writing - Review & Editing

Pavel Pleskunov: Visualization, Writing - Review & Editing

Andrei Choukourov: Writing - Original Draft, Writing - Review & Editing

Declaration of interests

☒ The authors declare that they have no known competing financial interests or personal relationships that could have appeared to influence the work reported in this paper.

☐The authors declare the following financial interests/personal relationships which may be considered as potential competing interests: